Macromolecules

pubs.acs.org/Macromolecules
Article

Synthesis of Oxazoline/Methacrylate-Based Graft-Copolymers *via* Grafting-Through Method and Evaluation of Their Self-Assembly in Water and Dodecane

Matilde Concilio, Nga Nguyen, Stephen C. L. Hall, Steven Huband, and C. Remzi Becer*

Cite This: *Macromolecules* 2023, 56, 7961−7972
Read Online

ABSTRACT: Well-defined graft-copolymers of poly(2-ethyl-2-oxazoline)methacrylate macromonomer (PEtOxMM), *n*-butyl methacrylate, and *n*-lauryl methacrylate were synthesized *via* the grafting-through method. The effect of composition on the thermal properties and solution behavior was investigated. Differential scanning calorimetry and thermogravimetric analysis showed little dependency of the thermal properties on the terpolymer composition, while the solution properties were found to be strongly dependent. Varying the PEtOxMM content, the resulting graft- copolymers were found to be soluble in water or *n*-dodecane. A thermoresponsive behavior was observed only for the graft-copolymers in water, as shown by turbidity measurements and dynamic light scattering analysis. Small-angle X-ray scattering measurements at different temperatures were performed to investigate the self-assembly behavior of the graft-copolymers in both *n*-dodecane and water. A range of temperature-triggered morphological transitions was observed in both solvents depending on the graft-copolymer composition. These graft-copolymers were able to self-assemble into different morphologies in both *n*-dodecane and water, exhibiting a high temperature stability.

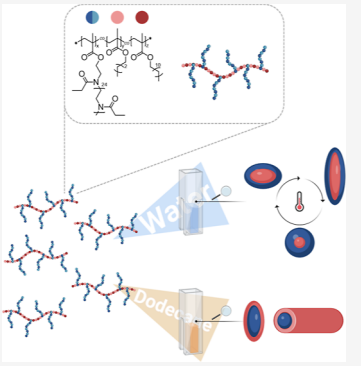

INTRODUCTION

The properties and conformation of graft-copolymers depend on various parameters, such as the grafting density, the flexibility (or rigidity) of the backbone, and the chemical composition.[1] Among all of these, the grafting density has the greatest effect on the final properties and conformation. On one hand, densely grafted side chains on a linear backbone result in steric repulsion between adjacent grafts and, consequently, in an increase in the main chain stiffness and in the hindrance of entanglements with neighboring polymer chains. As a result, these macromolecules form with a cylindrical or bottlebrush-like structure, with backbone flexibility on the scale of the distance between neighboring grafts.[2] At length scales longer than the side-chain length, the macromolecules behave like semiflexible cylinders. On the other hand, flexible comb-like polymers, characterized by a low grafting density, exhibit a Gaussian chain behavior for both side and main chains.[3]

The distinct molecular characteristics of graft-copolymers and the ability of combining the properties of different polymeric units within the same macromolecule have opened the possibility of a variety of novel potential applications that could not be achieved with linear (co)polymers.[4] This became possible due to the development of advanced synthetic techniques, which enabled a precise control over a range of parameters, including the grafting density and the side-chain length. Graft-copolymers are most frequently synthesized *via* three methods: grafting-through, grafting-from, and grafting-onto approaches.[5]

The combination of hydrophilic and hydrophobic monomers into well-defined polymers with specific macromolecular architectures results in amphiphilic compounds, which can self-assemble in solution into nanoscale-sized objects.[6] The solution self-assembly of amphiphilic copolymers has been widely investigated in the literature, especially for block copolymers, which can self-assemble into various well-defined morphologies.[7] Furthermore, the self-assembly behavior of polymers in solution can be triggered by external stimuli, such as temperature, light, pH, mechanical forces, magnetic fields, and other chemical stimuli.[8] Among all, temperature remains the most employed trigger for the design of stimuli-responsive polymers, predominantly in aqueous media, as can be observed from the plethora of available review articles summarizing their synthesis and applications, mainly in the biomedical field.[9]

Poly(2-oxazoline)s have recently emerged as a powerful class of polymers with various potential applications due to their relatively easy synthesis and their chemical and structural designability. The cationic ring-opening polymerization (CROP) of 2-oxazolines results in the synthesis of well-defined (co)polymers, whose end-group functionalities can be con-

Received: July 3, 2023
Revised: August 26, 2023
Published: September 25, 2023

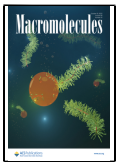

https://doi.org/10.1021/acs.macromol.3c01308
Macromolecules 2023, 56, 7961−7972

trolled during the initiation and termination steps and whose properties can be easily tuned by varying the length of the alkyl side chains on the 2-oxazoline monomer.[10] Furthermore, poly(2-oxazoline)s can be easily incorporated into more complex architectures, resulting in further control over their properties.

Examples of well-defined brush and grafted architectures containing 2-oxazolines synthesized *via* the *grafting-through*,[11] *grafting-from*,[12] and *grafting-onto* approaches are present in the literature,[13−15] evidencing the great versatility of this monomer class. In the past decade, the focus of research into the self-assembly of 2-oxazoline graft-copolymers has been investigated in aqueous solutions. Depending on the self-assembly technique used, the composition, and the hydrophobic/hydrophilic balance of the 2-oxazoline-based graft-copolymers, spherical and worm-like micelles,[16] vesicles,[17] and more complex morphologies,[18] such as multicompartment micelles and vesicles, could be obtained. Furthermore, because of the well-known thermoresponsive behavior of poly(2-oxazoline)s,[19] temperature-triggered self-assembly behaviors and morphological transitions of 2-oxazoline graft-copolymers have also been investigated. For example, a temperature-triggered morphological transition was observed for grafted copolymers consisting of a linear poly(ethylene imine) backbone and poly(2-ethyl-2-oxazoline) (PEtOx) side chains.[15] Depending on the grafting density and the length of both the backbone and the side chains, the graft-copolymers were able to self-organize into ordered structures with different morphologies and internal structures. Upon heating, a change in morphology was observed due to the thermoresponsive behavior of PEtOx. By carefully varying the polymer composition and the temperature, rodlike anisotropic particles, compact cylindrical aggregates with circular cross sections, core−shell cylinders, and core−shell spheres could be obtained.[15] Recently, thermoresponsive graft-copolymers consisting of a polypeptide backbone and poly(oxazoline) side chains showed temperature-induced phase transitions in water due to the presence of the thermoresponsive oxazoline units.[20,21] For example, graft-copolymers consisting of a poly(tyrosine) backbone and PEtOx side chains, exhibiting a lower critical solution temperature (LCST) behavior in water, could self-assemble into micelles consisting of a hydrophobic polypeptide core and hydrophilic PEtOx corona below their cloud point temperature (T_{CP}) and formed micellar aggregates above T_{CP}.[21]

However, it is important to note that the study and understanding of the self-assembly behavior of statistical amphiphilic copolymers and, in particular, of statistical graft-copolymers, are still limited. As in the case of diblock copolymers, amphiphilic statistical copolymers can self-assemble into a wide range of morphologies, including spheres,[22,23] cylindrical micelles,[24] vesicles,[23,25] and bowl-shaped structures.[26] Therefore, in this study, the synthesis of well-defined statistical graft-copolymers based on 2-oxazoline and methacrylate monomers *via* the grafting-through approach is reported. The graft-copolymers are obtained *via* reversible addition−fragmentation chain-transfer (RAFT) polymerization of a poly(2-ethyl-2-oxazoline)methacrylate macromonomer with *n*-lauryl methacrylate and *n*-butyl methacrylate. The final polymer composition is systematically varied to evaluate the effect on the thermal properties and solution behavior of the graft-copolymers. The study of the thermoresponsive behavior and self-assembly of the graft-copolymers in water and dodecane is first assessed by turbidity measurements and light scattering techniques. Small-angle X-ray scattering (SAXS) measurements at different temperatures are employed to investigate the self-assembly behavior of the graft-copolymers in both solvents.

RESULTS AND DISCUSSION

Synthesis of Poly(2-ethyl-2-oxazoline) Macromonomer (PEtOxMM). In the grafting-through approach (or the macromonomer method), a low-molecular-weight monomer is polymerized with a (meth)acrylate-functionalized macromonomer, resulting in graft-copolymers bearing well-defined side chains.[27] In this study, a poly(2-ethyl-2-oxazoline) macromonomer (PEtOxMM) was synthesized *via* CROP of 2-ethyl-2-oxazoline (EtOx) and subsequently end-capped with methacrylic acid, yielding a methacrylate-functionalized final polymer. The CROP of EtOx was carried out in acetonitrile (CH_3CN) at 100 °C using methyl tosylate (MeTos) as the initiator (Scheme 1). The [monomer] to [MeTos] ratio was 25:1.

Scheme 1. Reaction Scheme of the Synthesis of the 2-Ethyl-2-oxazoline Macromonomer (PEtOxMM)[a]

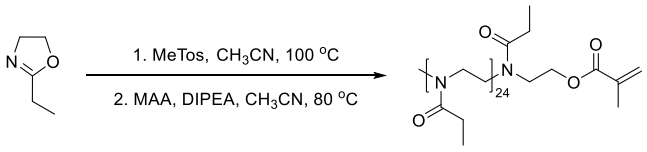

[a]MeTos = methyl tosylate, MAA = methacrylic acid, DIPEA = *N*, *N* diisopropylethylamine.

After reaching full EtOx conversion, a solution containing fivefold excess of methacrylic acid and *N*, *N*-diisopropylethylamine (DIPEA) in CH_3CN was directly added to the sealed vial containing the living oxazoline chains. The methacrylate anions generated *in situ* in the presence of DIPEA directly end-capped the polymer chains bearing living oxazolinium species. ^{1}H NMR spectroscopy was employed to evaluate the efficiency of the end-capping reaction after the purification of the resulting macromonomer to remove the excess reagents (Figure S1).

The PEtOxMM macromonomer showed a narrow molecular weight distribution ($\bar{M}_{n,th}$ = 2578 g mol^{-1}, $\bar{M}_{n,GPC}$ = 2400 g mol^{-1}, $Đ$ = 1.10), which is expected from a controlled living polymerization (Figure S2). Because of the difference in hydrodynamic volume between the PMMA standards used in the GPC calibration and that of the macromonomer, a discrepancy between the theoretical and experimental molecular weight distributions was expected.

Synthesis of Oxazoline/Methacrylate Graft-Copolymers *via* the Grafting-Through Method. The second step of the graft-copolymer synthesis *via* the grafting-through approach is the copolymerization of the macromonomer with low-molecular-weight monomers. In this case, PEtOxMM was copolymerized with two hydrophobic methacrylates, namely, *n*-butyl methacrylate (BuMA) and *n*-lauryl methacrylate (LMA), *via* RAFT polymerization (Scheme 2). 2-Cyano-2-propyl benzodithioate (CPBD) was employed as the chain-transfer agent and dimethyl 2,2′-azobis(2-methylpropionate) (V-601) as the initiator.

For all synthesized terpolymers, the polymerization was performed at a monomer concentration of 0.5 M in chloroform ($CHCl_3$) at 70 °C. In order to evaluate the effect of the composition on the properties of the final graft-copolymers,

https://doi.org/10.1021/acs.macromol.3c01308
Macromolecules 2023, 56, 7961−7972

Scheme 2. Schematic Representation of the Synthesis of Graft-Copolymers *via* the Grafting-Through Approach by RAFT Polymerization of Butyl Methacrylate (BuMA), Lauryl Methacrylate (BuMA), and PEtOxMM

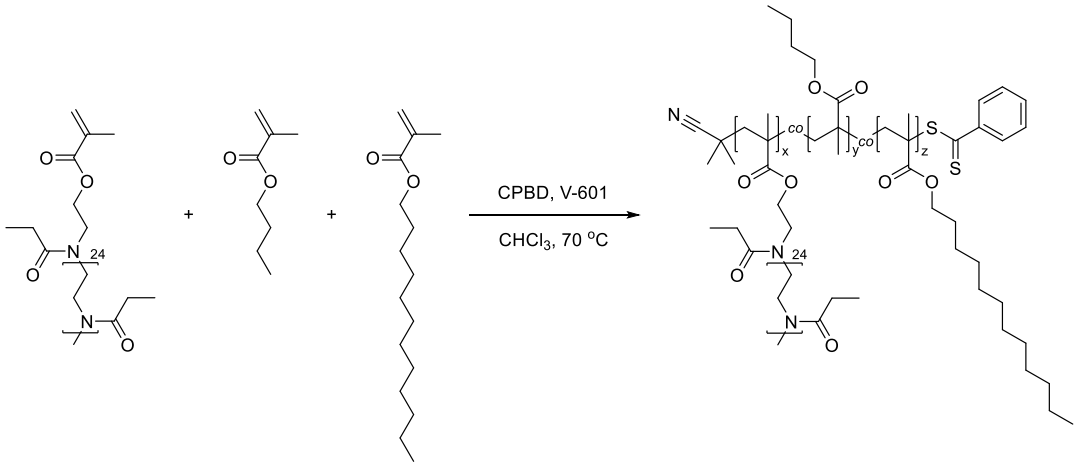

Table 1. Graft-Copolymers of PEtOxMM, BuMA, and LMA Obtained *via* the Grafting-Through Approach

sample	$[PEtOxMM/BuMA/LMA]_{initial}$ [a]	conversion (%)			$[PEtOxMM/BuMA/LMA]_{final}$ [d]	$\bar{M}_{n,th}$ (g mol^{-1})	$\bar{M}_{n,SEC}$ [e] (g mol^{-1})	$Đ$
		PEtOxMM[b]	BuMA[c]	LMA[c]				
GP1	9:43:47	88	>99	>99	8:43:47	38,925	25,900	1.17
GP2	9:55:32	87	>99	>99	8:55:32	36,815	26,600	1.17
GP3	9:29:64	86	>99	>99	8:29:64	41,259	27,500	1.19
GP4	16:38:41	83	>99	>99	13:38:41	49,583	30,700	1.19
GP5	17:48:28	81	>99	>99	14:48:28	50,276	29,000	1.20
GP6	17:27:58	81	>99	>99	14:27:58	54,923	29,900	1.21
GP7	25:42:43	86	>99	>99	22:42:43	73,871	33,200	1.18
GP8	25:44:27	88	>99	>99	22:44:27	70,085	35,100	1.14
GP9	25:27:54	86	>99	>99	22:27:54	74,537	35,100	1.21

[a]Determined from ^{1}H NMR spectra at t_0. [b]Determined by GPC measurements. [c]Determined by ^{1}H NMR spectroscopy. [d]Final polymer composition calculated from the monomer conversion. [e]Measured in THF with 2% TEA using PMMA standards and a single column.

three series of terpolymers were synthesized. The PEtOxMM equivalents were kept fixed to 8, 14, or 22 equiv, while the ratio between BuMA and LMA was systematically varied to a theoretical composition of 30:70, 50:50, and 70:30 (Table 1). The exact initial monomer feed ratio, $[PEtOxMM/BuMA/LMA]_{initial}$, was calculated from the ^{1}H NMR spectrum of each terpolymer before starting the polymerization, as shown in an example NMR spectrum (Figure S3). A total of nine grafted terpolymers were obtained. The overall [monomer]/[CPDB]/[V-601] ratio was kept constant at 100:1:0.25 for all terpolymers. To increase the conversion of the PEtOx macromonomer, 0.12 equiv of the initiator was further added to the reaction mixture after 48 h from the beginning of the polymerization. The reaction mixture was kept at 70 °C for further 24 h, for a total of 72 h.

At the end of the polymerization, the BuMA and LMA conversions were determined from the ^{1}H NMR spectra (Figures S4 and S5), while the PEtOxMM conversion was calculated from the GPC curves using the integration method, as already reported in the literature (Figure S6).[13]

Subsequently, the terpolymers were purified by dialysis in water for 10 days and analyzed by ^{1}H and ^{1}H−^{13}C HSQC NMR spectroscopy to monitor the complete removal of the unreacted water-soluble PEtOxMM (Figures 1 and S7). ^{1}H−^{13}C HSQC spectroscopy was used to resolve the overlapping signals and to detect the presence of a small amount of unreacted PEtOxMM. As can be observed in Figure 1B, the peaks obtained in the ^{1}H NMR spectrum correspond only to proton−carbon correlations related to the grafted terpolymer, and no correlations were found for the unreacted macromonomer, indicating its complete removal.

GPC analysis of the graft-copolymers **GP1−GP9** after dialysis showed unimodal molecular weight distributions with narrow dispersities (Figure 2). Due to the difficulty in discerning the peaks related to PEtOx, BuMA, and LMA in the ^{1}H NMR spectra for the determination of the kinetics of the polymerization of the three compounds, kinetic studies were performed on the individual copolymerizations of BuMA/LMA, BuMA/PEtOxMM, and LMA/PEtOxMM. The determination of the reactivity ratios and the calculation of their products suggested the synthesis of pseudogradient diblock graft-copolymers. The graft-copolymers consisted of an initial BuMA-enriched statistical region, followed by a gradient domain of the three methacrylates and, finally, an LMA-enriched statistical region, whose composition depended on the monomer feed ratio (Table S4 and Figure S8).

Determination of the Thermal Properties of the Graft-Copolymers. The thermal stability of the copolymers was evaluated *via* thermogravimetric analysis (TGA). The polymers were heated from 25 to 550 °C at a heating rate of 10 °C min^{-1} under air. All polymers showed thermal stability up to 200 °C with similar thermal decomposition profiles (Figure S9).

Subsequently, the thermal properties of the copolymers were investigated *via* differential scanning calorimetry (DSC). A first

https://doi.org/10.1021/acs.macromol.3c01308
Macromolecules 2023, 56, 7961−7972

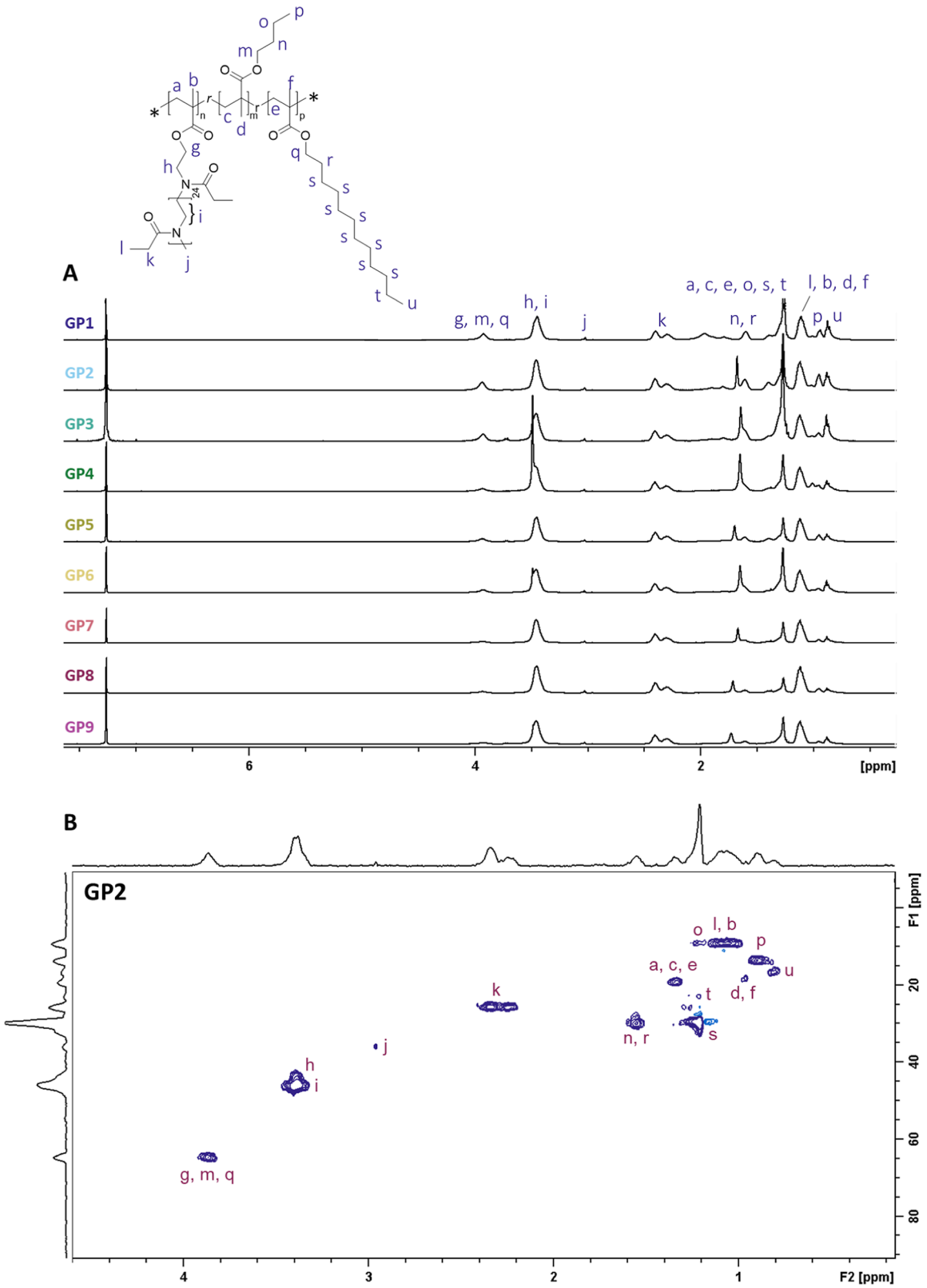

Figure 1. (A) ^{1}H NMR spectra (400 MHz, $CDCl_3$) of **GP1**−**GP9** after dialysis, showing the absence of the PEtOxMM peaks at 5.4−6.2 ppm and (B) HSQC spectrum (400 MHz, $CDCl_3$) of **GP2**, demonstrating the complete removal of the unreacted PEtOxMM. For brevity, the end-groups of the graft-copolymer are not shown in the chemical structure.

fast heating/cooling cycle from −40 to 140 °C at 60 °C min^{-1} under nitrogen atmosphere was used to remove the thermal history of the samples, followed by two further heating/cooling cycles from −40 to 140 °C at 20 °C min^{-1}.

The DSC curves of the terpolymers showed a single thermal transition, corresponding to a glass transition (Figure S10). The measured glass transition temperatures (T_g) showed values between the T_g of the EtOx macromonomer and the BuMA

https://doi.org/10.1021/acs.macromol.3c01308
Macromolecules 2023, 56, 7961−7972

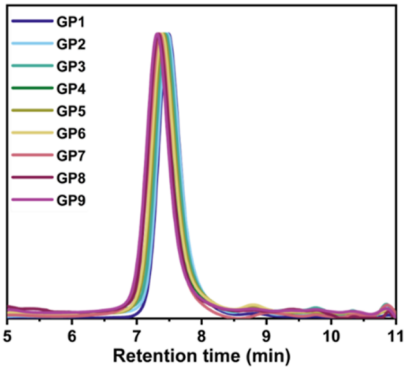

Figure 2. GPC traces of **GP1**−**GP9** after purification using THF with 2% TEA as an eluent.

homopolymer (Table 2). However, a trend was not observed since the **GP1**−**GP9** graft-copolymers exhibited T_g values in the same range (30−36 °C). The measured T_g values were not dependent on the final chemical composition, probably due to the statistical incorporation of the monomers within the polymer chains. However, it is important to note that the terpolymers presented only one thermal transition and not two, providing more evidence of the formation of statistical or gradient copolymers and not of block copolymers.

Table 2. Glass-Transition Temperatures ($T_{g,exp}$) Obtained from the DSC Analysis of the BuMA and LMA Homopolymers, PEtOxMM, and GP1−GP9 Graft-Copolymers

sample	$(PEtOxMM/BuMA/LMA)_{exp}$	$T_{g,exp}$ (°C)
PBuMA	0:102:0	20
PLMA	0:0:94	
PEtOxMM	EtOx DP 25	44
GP1	8:43:47	35
GP2	8:55:32	35
GP3	8:29:64	36
GP4	13:38:41	31
GP5	14:48:28	30
GP6	14:27:58	32
GP7	22:42:43	33
GP8	22:44:27	35
GP9	22:27:54	36

Evaluation of the Thermoresponsive Behavior of the Graft-Copolymers *via* Transmittance Measurements. The solution behavior of the terpolymers was investigated in both water and dodecane in order to evaluate the effect of the chemical composition on the final solution properties in two solvents with very different polarities.

Solubility tests of the terpolymers in water and dodecane were first performed by dissolving the polymers at a concentration of 5 mg mL^{-1}. The terpolymers containing a high amount of PEtOxMM (*i.e.*, **GP4**−**GP9**) were only soluble in water, while the terpolymers with the lowest PEtOxMM content (*i.e.*, **GP1** and **GP3**) were only soluble in dodecane (Table S5). Interestingly, **GP2** did not form a transparent solution in either of the two solvents, suggesting that a high content of LMA was necessary to achieve solubility in dodecane.

Afterward, the solution behavior of the terpolymers was investigated *via* UV−vis spectroscopy. Poly(2-ethyl-2-oxazoline) has a well-known thermoresponsive behavior in water, exhibiting an LCST between 60 and 63 °C, depending on the polymer molecular weight and concentration.[28] Consequently, the copolymerization of PEtOxMM with hydrophobic monomers should decrease the overall T_{CP} to lower values. Moreover, in the case of the dodecane-soluble terpolymers, the inclusion of LMA in the composition might induce an upper critical solution temperature (UCST) behavior due to the crystallization of the alkyl chains, as previously reported for other polymers.[29]

The dodecane-soluble graft-copolymers **GP1** and **GP3** were first analyzed at a concentration of 5 mg mL^{-1}. The samples were subjected to two heating/cooling cycles from 15 to 85 °C at a heating rate of 1 °C min^{-1}. As can be observed in Figure S11, the graft-copolymers were completely soluble in dodecane and did not show any thermoresponsive behavior, as indicated by transmittance values close to 100% over the whole analyzed temperature range. This suggested that the alkyl chains of the LMA units might not have been long enough to form crystalline domains, which could have been solubilized upon heating. Alternatively, the statistical distribution of the LMA monomer along the polymer chains, together with the long PEtOx side chains, might have hindered the packing of the LMA alkyl chains into crystalline domains. Finally, the BuMA units might have disrupted the packing due to the presence of short alkyl chains, which probably remained noncrystalline at higher temperatures.

On the contrary, the water-soluble graft-copolymers exhibited an LCST behavior in water, which was dependent on the polymer chemical composition and on the polymer concentration. At 5 mg mL^{-1}, the T_{CP} values of the terpolymers containing 14 equiv of PEtOxMM (*i.e.*, **GP4**−**GP6**) were dependent on the content of the most hydrophobic monomer, LMA (Figure 3A). For instance, a slight decrease in T_{CP} from 64, to 62, to 60 °C was observed with the increasing LMA content from 28 equiv (**GP5**), to 41 equiv (**GP4**), to 58 equiv (**GP6**), respectively. As expected for polymer solutions, a hysteresis between the T_{CP} values of the heating and cooling curves was observed for all terpolymers (Figure 3C). This phenomenon was less pronounced for **GP6**, containing the highest amount of LMA units, due to its more hydrophobic nature compared to **GP4** and **GP5**.

In the case of **GP7**−**GP9** with 22 equiv of PEtOxMM, this trend was less pronounced, with the terpolymers showing similar T_{CP} values at around 67 °C during the heating cycle (Figure 3B). The overall hydrophobicity of the terpolymers might not have been enough compared to the high PEtOxMM content to induce a decrease in the T_{CP} values with increasing LMA content, as observed for **GP4**−**GP5**. In this case, a narrower hysteresis compared with **GP4**−**GP6** was observed (Figure 3D).

The dependence of the thermoresponsive behavior on the polymer concentration was investigated by increasing the terpolymer concentration in water from 5 to 20 mg mL^{-1} (Figure S12). For all terpolymers, while the T_{CP} values for the cooling cycle remained invariant or decreased, as expected for more concentrated solutions, an increase in the hysteresis between the cycles was detected, indicating that at higher polymer concentrations the compounds required higher temperatures to precipitate during the heating cycle. This might have been caused by the formation of high-ordered structures, as a consequence of their amphiphilic nature, which hindered their aggregation at lower temperatures.

Dynamic Light Scattering Analysis of the Self-Assembly Behavior of GP1−**GP9.** Since the combination of hydrophobic and hydrophilic moieties in the same polymer chain could result in the self-assembly into high-order structures

https://doi.org/10.1021/acs.macromol.3c01308
Macromolecules 2023, 56, 7961−7972

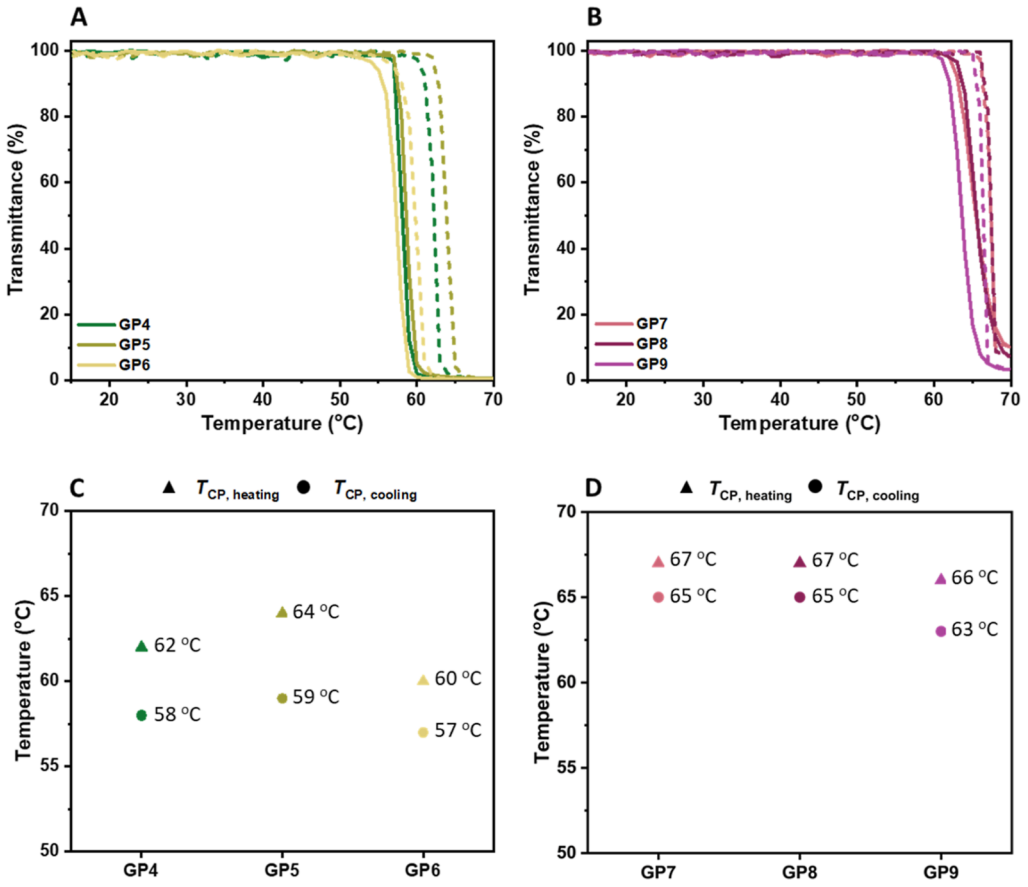

Figure 3. Transmittance curves of the second heating (dashed line) and cooling (solid line) cycles of 5 mg mL^{-1} polymer solutions in water of terpolymers containing (A) 14 and (B) 22 equiv of PEtOxMM. T_{CP} values calculated at 50% transmittance during the heating (triangle) and cooling (circle) cycles of terpolymers containing (C) 14 and (D) 22 equiv of PEtOxMM.

of the polymer in solution, the graft-copolymers were analyzed *via* dynamic light scattering (DLS) measurements in water and dodecane depending on their solubility.

The thermoresponsive copolymers (**GP4**−**GP9**) were dissolved in water at a polymer concentration of 20 mg mL^{-1}, and the particle size was determined at 25 °C and at a higher temperature just before the phase transition of each compound, as previously measured by transmittance measurements (Figures S13 and S14). For the dodecane-soluble terpolymers, **GP1** and **GP3**, the measurements were performed at 25 and 70 °C to evaluate if temperature would have an effect on their self-assembly behavior. In this case, the concentration was decreased to 12 mg mL^{-1} since the polymers were not completely soluble in dodecane at higher concentrations.

Interestingly, **GP1**, containing a lower amount of LMA and a higher amount of BuMA, formed bigger particles (∼33 nm) at 25 °C than the more hydrophobic **GP3** (∼18.2 nm), as reported in Table S6. At 70 °C, the hydrodynamic diameter of the two terpolymers did not significantly change, suggesting that the increase in temperature did not have an effect on their self-assembly behavior.

On the contrary, the DLS analyses of the terpolymers soluble in water confirmed the existence of the thermoresponsive behavior, as already demonstrated by transmittance measurements (Table S6). An increase in the size of the particles was detected for all terpolymers at temperatures close to their T_{CP} values, where the solutions were still transparent and no cloudiness was visually detected. In the case of the graft-copolymers containing 14 equiv of PEtOxMM, the particle size was dependent on the LMA content, with the formation of bigger particles with increasing LMA content, from 17.4 nm for **GP5**, to 21.4 nm for **GP4**, to 35.4 nm for **GP6**. As expected, the particle size increased with temperature, resulting in particles with hydrodynamic diameters of 20.5, 28.5, and 43.3 nm for **GP5**, **GP4**, and **GP6**, respectively. This trend was also observed for the graft-copolymers containing 22 equiv of PEtOxMM, which showed hydrodynamic diameters of 13.0, 14.2, and 15.0 nm for **GP8**, **GP7**, and **GP9** at 25 °C, respectively. The increase in temperature resulted in the formation of larger particles with sizes of 19.0 nm for **GP8**, 20.9 nm for **GP7**, and 18.2 nm for **GP9**.

It is important to note that due to the small dimensions of the obtained aggregates, self-assembly might also refer to the folding of an individual polymer chain into a single-chain nanoparticle. However, further analyses need to be performed to gain more insights about the observed behavior.

Small-Angle X-ray Scattering Analysis of the Self-Assembly Behavior of GP1−GP9. In order to gain insights into the morphology and internal structure of the polymer assemblies observed by DLS, SAXS was used as a nondestructive technique. The aqueous polymer solutions of **GP4**−**GP9** were prepared at a concentration of 20 mg mL^{-1}, while the dodecane solutions of **GP1** and **GP3** were prepared at 12 mg mL^{-1}. As for the DLS measurements, the samples were analyzed at room temperature and at a high temperature.

https://doi.org/10.1021/acs.macromol.3c01308
Macromolecules 2023, 56, 7961−7972

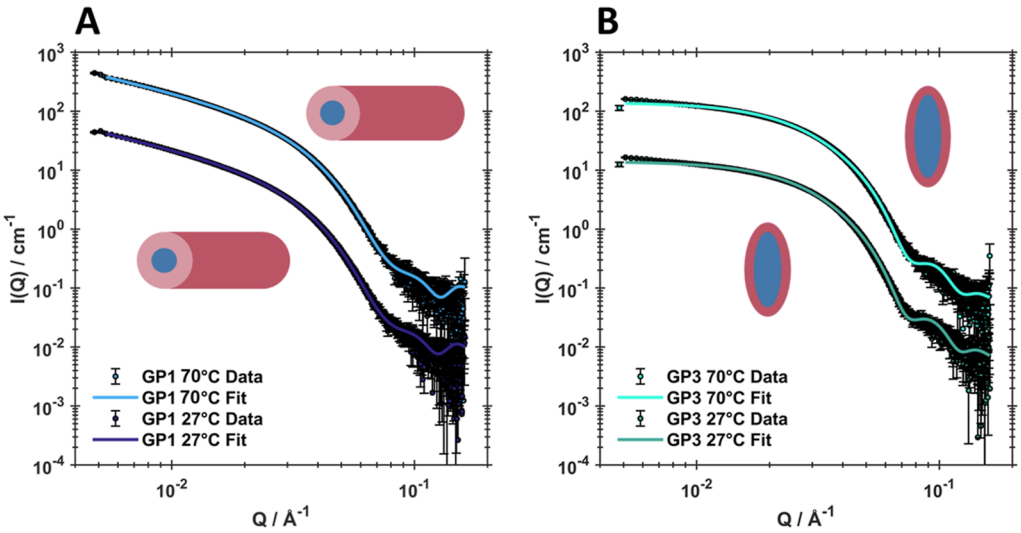

Figure 4. SAXS data (points) and associated structural fits (lines) for (A) **GP1** and (B) **GP3** measured at 27 and 70 °C. Data collected at higher temperatures have been vertically offset by a factor of 10 to aid clarity.

For the **GP1** and **GP3** graft-copolymers analyzed at 27 °C in dodecane, a significant difference between the scattering patterns could be especially observed at low values of Q, where the decay in scattering intensity showed different gradients (Figure 4). In the case of **GP1**, the decay in intensity followed a Q^{-1} decay, indicating the formation of cylindrical particles. Here, best fits to the data were achieved by using a core−shell cylindrical form factor. In the case of **GP3**, Q^{-1} decay in scattering intensity at low Q was not observed. This suggested the formation of less elongated particles, where best fits to the data were achieved using a form factor describing core−shell prolate ellipsoidal particles.

In the case of **GP1**, the total length of these core−shell cylinders was not determinable within the achievable Q range, and consequently, it was kept fixed throughout the analysis. Nevertheless, these structures were characterized by a core radius of around 3.3 nm and a shell thickness of around 4.1 nm (Table 3).

It is worth noting that the SLD of the core was higher than what would be expected for PEtOx in a good solvent. This suggested that there was a higher electron density in the core, indicating that PEtOx chains were collapsed and densely packed together, driven by their insolubility in dodecane. Therefore, it is suggested that the cylinders consisted of a dense core of aggregated PEtOx chains surrounded by a stabilizing dodecane-soluble BuMA−LMA shell.

By increasing the amount of LMA in the graft-copolymer, a change in morphology was observed, as reported for LMA-containing diblock copolymers in *n*-alkanes.[30] The data suggested the formation of core−shell prolate ellipsoids with a core radius of ∼3.6 nm, a core polar radius of ∼9.8 nm, and a shell thickness of ∼2.5 nm. It is worth mentioning that, in this case, the core SLD was considerably lower than the core SLD of **GP1**, suggesting that either the core contained a large amount of solvent or that the core−shell structure was not particularly defined. This could indicate that the core consisted not only of pure PEtOx segments but also of a mixed phase containing BuMA and LMA segments. A change in morphology depending on the amount of the most hydrophobic monomer has been observed.

Table 3. Parameters Obtained through Fitting the SAXS Data for the Dodecane-Soluble Samples to Models Consisting of Cylinders with a Core−Shell Structure (GP1) and Ellipsoid Particles with a Core−Shell Structure (GP3) Form Factor[a]

	GP1	
cylinders	27 °C	70 °C
$\rho_{Core}/\times10^{-6}$ Å^{-2}	11.52 ± 0.02	11.60 ± 0.02
core radius/Å	32.7 ± 0.2	32.0 ± 0.2
shell thickness/Å	41.4 ± 0.1	40.2 ± 0.1
length/Å	2000	2000
core radius polydispersity	0.12 ± 0.01	0.12 ± 0.01
	GP3	
core−shell ellipsoids	27 °C	70 °C
$\rho_{Core}/\times10^{-6}$ Å^{-2}	8.68 ± 0.01	8.73 ± 0.02
core equatorial radius/Å	35.8 ± 1.0	36.4 ± 1.2
core polar radius/Å	98.45 ± 3.28	109.2 ± 4.4
shell thickness/Å	24.8 ± 0.9	23.5 ± 1.0
core radius polydispersity	0	0

[a]SLD of the core (ρ_{core}), core radius, core equatorial radius, core polar radius, shell thickness, length, and core radius polydispersity were extracted from the fits. More detailed descriptions can be found in Tables S1 and S2 (Supporting Information).

For both graft-copolymers, similar structural parameters were observed in the data measured at 70 °C, in agreement with the DLS measurements, indicating that temperature did not cause a change in morphology, as instead reported for other LMA-containing diblock copolymers in dodecane.[31] The results also highlighted the high stability of these assemblies even at a high temperature.

The **GP4−GP9** graft-copolymers in water exhibited higher core SLD compared to the SLD of statistical BuMA−LMA copolymers at both low and high temperatures (Table 4). This suggested the formation of very compact and dense cores consisting of BuMA and LMA segments that collapsed to minimize their contact with water.

The graft-copolymers with 14 equiv of PEtOxMM (**GP4−GP6**) were first analyzed. At room temperature, **GP4** and **GP5** exhibited similar scattering patterns, with a core axial ratio lower than 1, indicating the formation of oblate, disk-like particles with

https://doi.org/10.1021/acs.macromol.3c01308
Macromolecules 2023, 56, 7961−7972

Table 4. Parameters Obtained through Fitting SAXS Data for GP4−GP9 Samples to the Model Consisting of an Ellipsoid Particle with a Core−Shell Structure Form Factor[a]

	GP4		GP5		GP6		GP7		GP8		GP9	
	27 °C	60 °C	27 °C	60 °C	27 °C	55 °C	27 °C	65 °C	27 °C	65 °C	27 °C	60 °C
$\rho_{Core}/\times10^{-6}$ Å^{-2}	9.82 ± 0.12	9.56 ± 0.01	9.43 ± 0.01	9.46 ± 0.003	9.55 ± 0.01	9.52 ± 0.004	9.63 ± 0.09	9.48 ± 0.01	9.44 ± 0.02	10.00 ± 0.25	9.57 ± 0.02	10.28 ± 0.23
core equatorial radius/Å	50.8 ± 2.3	34.1 ± 1.0	57.9 ± 1.5	40.3 ± 0.9	40.5 ± 0.6	42.5 ± 0.6	26.3 ± 2.6	30.2 ± 1.7	31.9 ± 1.5	10.6 ± 2.3	30.5 ± 1.2	16.8 ± 1.8
core polar radius/Å	15.24 ± 2.15	166.41 ± 6.37	31.27 ± 1.41	128.96 ± 3.76	158.76 ± 3.38		26.3 ± 2.6	168.52 ± 12.12	31.9 ± 1.5	105.79 ± 29.92	55.21 ± 2.49	71.40 ± 9.65
shell thickness/Å	52.4 ± 2.6	38.3 ± 1.3	31.7 ± 1.8	22.1 ± 1.2	36.7 ± 0.8	30.0 ± 0.8	44.7 ± 2.8	25.7 ± 2.1	28.5 ± 1.8	40.2 ± 2.9	36.8 ± 1.5	48.2 ± 2.1
core radius polydispersity	0	0	0	0	0	0.19 ± 0.004	0.06 ± 0.02	0	0.17 ± 0.01	0.42 ± 0.05	0	0

[a]SLD of the core (ρ_{core}), core equatorial radius, core polar radius, shell thickness, and core radius polydispersity extracted from the fits. More detailed descriptions can be found in Table S3 (Supporting Information).

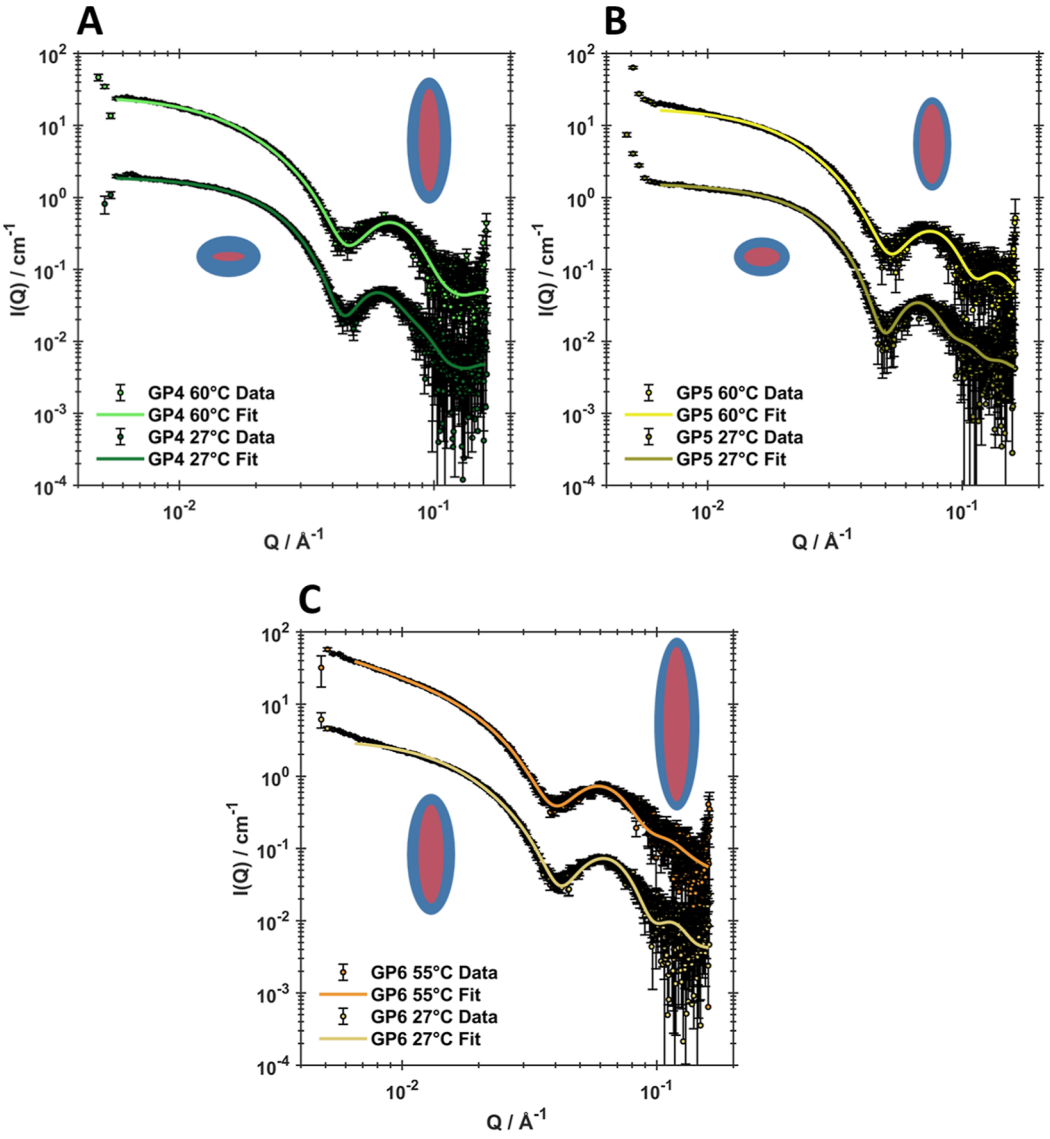

Figure 5. SAXS data (points) and the associated structural fits (lines) for (A) **GP4**, (B) **GP5**, and (C) **GP6** measured in water at 27 °C and at high temperature. Data collected at a higher temperature have been vertically offset by a factor of 10 to aid clarity.

core equatorial radii of 5.1 and 5.8 nm, respectively, and core polar radii of 1.5 and 3.1 nm, respectively (Figure 5A,B). While still self-assembling into oblate ellipsoids, **GP5** exhibited a more spherical morphology, probably due to the less compact structure of the core caused by the lower hydrophobicity of BuMA compared to LMA. This was also suggested by the lower value of the core SLD and a larger core polar radius. Furthermore, the thickness of the PEtOx shell was thinner

https://doi.org/10.1021/acs.macromol.3c01308
Macromolecules 2023, 56, 7961−7972

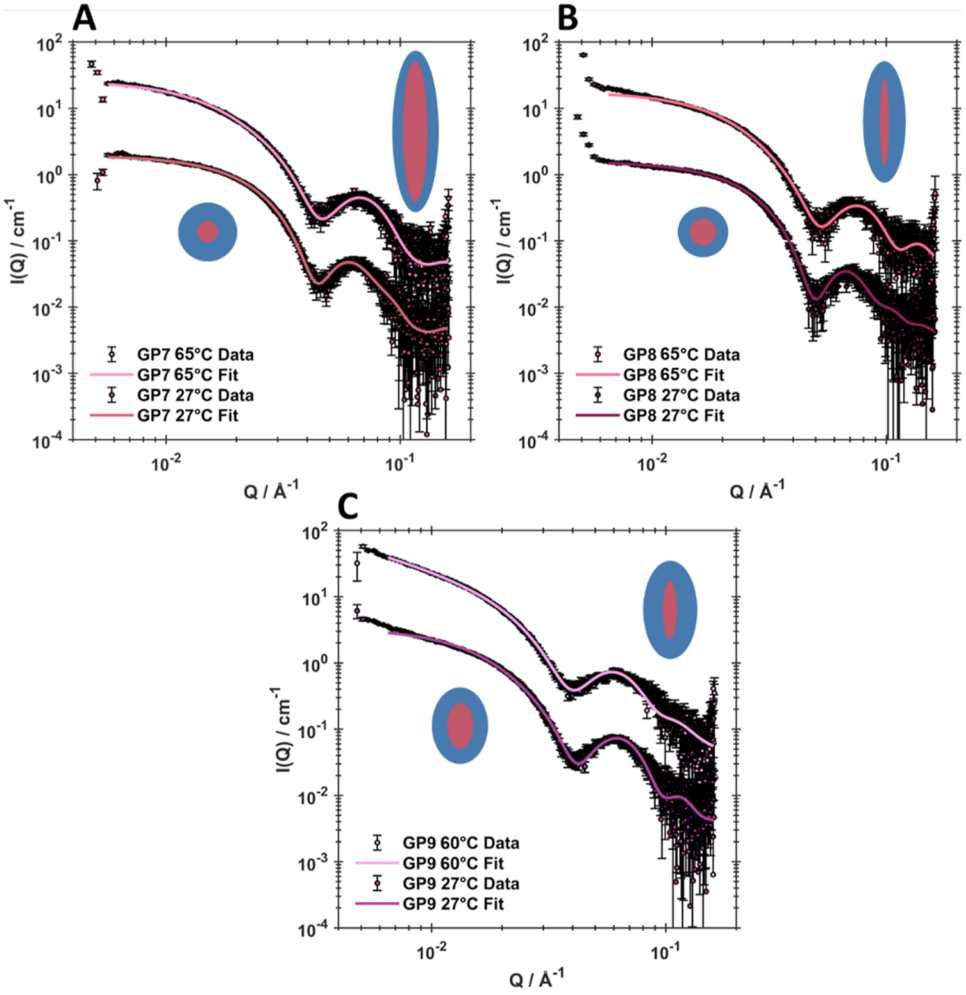

Figure 6. SAXS data (points) and associated structural fits (lines) for (A) **GP7**, (B) **GP8**, and (C) **GP9** measured in water at 27 °C and high temperature. Data collected at higher temperatures have been vertically offset by a factor of 10 to aid clarity.

compared with that of **GP4**, with values of 3.2 and 5.2 nm, respectively. Interestingly, the increase in temperature resulted in a change in morphology from oblate to prolate particles, as demonstrated by an increase in the core polar radius to ∼16.6 nm for **GP4** and ∼12.9 nm for **GP5**. A reduction of the core equatorial radius from 5.1 to 3.4 nm for **GP4**, and from 5.8 to 4.0 nm for **GP5**, was also observed. A decrease in the thickness of the shell to 3.8 and 2.2 nm for **GP4** and **GP5**, respectively, was also detected. This was attributed to the thermoresponsive behavior of PEtOx, which led to a collapse of the polymer chains forming the corona.

Interestingly, a different scattering pattern was recorded for **GP6**, the graft-copolymer having the highest amount of LMA, compared to that of **GP4** and **GP5** (Figure 5C). For instance, a core axial ratio greater than 1 indicated the formation of prolate particles at both room and high temperatures, with the core equatorial radii of 4.1 and 4.3 nm, respectively. The increase in the equatorial axial core at a high temperature suggested the formation of elongated particles with longer lengths compared to the prolate particles formed at room temperature having a core polar radius of ∼15.9 nm. However, it should be noted that, as with the cylindrical particles formed by **GP1**, the length of the elongated particles formed by **GP6** could not be determined within the accessible *Q* range. Also in this case, a reduction of the thickness of the PEtOx shell from 3.7 to 3.0 nm was observed with the increasing temperature, suggesting a similar thermoresponsive collapse of PEtOx chains, as seen with **GP4** and **GP5**.

The increase in the content of PEtOxMM from 14 to 22 equiv resulted in graft-copolymer assemblies with different morphologies, as shown by the scattering patterns in Figure 6A−C. At room temperature, **GP7** and **GP8** exhibited a core axial ratio of 1, indicating the formation of core−shell spherical particles with radii of 2.6 and 3.2 nm, respectively. Also, in this case, the presence of a higher content of BuMA resulted in larger, less compacted cores. In the case of **GP9**, a core axial ratio greater than 1 suggested the formation of slightly prolate particles, with a core equatorial radius of 3.1 nm and a core polar radius of 5.5 nm.

The increase in temperature also resulted in a change of morphology for the **GP7**−**GP9** graft-copolymers. For instance, a spherical-to-prolate particle transition was observed for **GP7**. Interestingly, the particles formed at higher temperatures were characterized by a slightly bigger equatorial core radius compared to the one measured at room temperature (3.0 and 2.6 nm, respectively), while the thickness of the PEtOx shell decreased from 4.5 to 2.6 nm. As above, this was attributed to the LCST-type phase transition of the hydrophilic segments, which collapsed upon an increase in temperature. In the case of **GP8** and **GP9**, elongated particles were observed at high temperatures, as demonstrated by the high core axial ratio

https://doi.org/10.1021/acs.macromol.3c01308
Macromolecules 2023, 56, 7961−7972

values. For both graft-copolymers, the assemblies formed at high temperatures were characterized by a much smaller core equatorial radius compared to the particles obtained at room temperature (1.1 and 1.7 nm, respectively) and by larger core polar radii of 10.6 and 7.1 nm, respectively. Interestingly, a decrease in the thickness of the PEtOx corona upon an increase in temperature was not observed. The substantial increase in the core SLD for both **GP8** and **GP9** indicated the formation of a significantly dense and compact core, resulting from the change in morphology. However, to explain the underlying mechanism behind these interesting morphological changes, further investigation needs to be performed.

Given the statistical composition, the synthesized statistical copolymers showed unexpected self-assembly properties. Core−shell elliptical particles have already been reported for partially hydrolyzed bottlebrush copolymers obtained from the RAFT polymerization of styryl-containing PEtOx macromonomers.[20] However, SANS analysis revealed strong interactions between particles at a lower polymer concentration, and no changes in morphology were observed by varying the degree of hydrolysis or temperature. Therefore, the results obtained in this study demonstrated the unique ability of the graft-copolymers to self-assemble into defined structures upon direct dissolution in dodecane or water.

CONCLUSIONS

In conclusion, a library of well-defined oxazoline/methacrylate copolymers was synthesized using the grafting-through approach. The methacrylate macromonomer of poly(2-ethyl-2-oxazoline) was copolymerized *via* RAFT polymerization with butyl methacrylate and lauryl methacrylate, and the final composition was systematically varied.

The effect of the final composition on the thermal properties was evaluated by TGA and DSC analyses. The **GP1−GP9** grafted terpolymers showed thermal stability up to 200 °C, with similar thermal decomposition profiles. DSC measurements demonstrated the presence of a glass transition, with T_g values in the range 31−36 °C, in between the T_g values of the BuMA homopolymer and PEtOxMM.

The solubility of the copolymers was evaluated in water and dodecane. On the one hand, **GP1** and **GP3**, containing the lowest amount of PEtOxMM, were soluble in dodecane, where no thermoresponsive behavior was detected. On the other hand, the graft-copolymers having a high content of hydrophilic PEtOxMM were soluble in water. **GP4−GP9** exhibited an LCST-type phase transition, with T_{CP} values in the range 55−69 °C, depending on the LMA content and polymer concentration.

DLS studies of the polymer solutions in water and dodecane demonstrated the self-assembly of the copolymers into bigger aggregates. SAXS studies were performed to gain insights into the morphology and internal structure of the polymer assemblies. Depending on the composition, the graft-copolymers were able to self-assemble into a wide range of morphologies in both dodecane and water, with the formation of well-defined structures, as demonstrated by the low core radius polydispersities. In dodecane, the graft-copolymers aggregated into cylinders or prolate ellipsoids, which did not show any temperature-induced morphological changes, demonstrating the high stability of these polymer assemblies even at high temperatures. Depending on the content of PEtOxMM and the ratio between BuMA and LMA, the graft-copolymers self-assembled into spherical, oblate, or prolate particles at room temperature. Interestingly, in all cases, the increase in the temperature resulted in well-defined morphological transitions. Therefore, the morphology, and the solubility of the resulting assemblies can be readily adjusted to meet specific application requirements. This could be achieved by meticulous design of the graft-copolymers, where the selection of the ratio between the methacrylate monomers and the PEtOxMM plays a pivotal role.

ASSOCIATED CONTENT

Supporting Information

The Supporting Information is available free of charge at https://pubs.acs.org/doi/10.1021/acs.macromol.3c01308.

Materials and methods; synthesis procedures; SAXS measurements; ^{1}H NMR analysis; GPC analysis; kinetic plots; TGA analysis; DSC analysis; transmittance measurements; and DLS analysis (PDF)

AUTHOR INFORMATION

Corresponding Author

C. Remzi Becer − *Department of Chemistry, University of Warwick, Coventry CV4 7AL, U.K.;* orcid.org/0000-0003-0968-6662; Email: Remzi.Becer@warwick.ac.uk

Authors

Matilde Concilio − *Department of Chemistry, University of Warwick, Coventry CV4 7AL, U.K.*

Nga Nguyen − *Infineum USA, Linden, New Jersey 07036, United States*

Stephen C. L. Hall − *Rutherford Appleton Laboratory, ISIS Neutron and Muon Source, Didcot OX110QX, U.K.;* orcid.org/0000-0003-0753-5123

Steven Huband − *Department of Physics, University of Warwick, Coventry CV4 7AL, U.K.*

Complete contact information is available at: https://pubs.acs.org/10.1021/acs.macromol.3c01308

Author Contributions

M.C. conceived the study, performed most of the experiments, and composed the manuscript. S.H. conducted the SAXS measurements. S.C.L.H. refined the SAXS fittings. C.R.B. and N.N. contributed essential resources, oversaw all aspects of the study execution, and edited the manuscript. All authors contributed to the generation, analysis or interpretation of the data, and edited the manuscript.

Notes

The authors declare no competing financial interest.

ACKNOWLEDGMENTS

The authors are grateful to Infineum USA L. P. for funding this work.

REFERENCES

(1) Sheiko, S. S.; Sumerlin, B. S.; Matyjaszewski, K. Cylindrical molecular brushes: Synthesis, characterization, and properties. *Prog. Polym. Sci.* **2008**, *33* (7), 759−785.

(2) Saariaho, M.; Ikkala, O.; Szleifer, I.; Erukhimovich, I.; Ten Brinke, G. On lyotropic behavior of molecular bottle-brushes: A Monte Carlo computer simulation study. *J. Chem. Phys.* **1997**, *107* (8), 3267−3276.

(3) Nakamura, Y.; Wan, Y.; Mays, J. W.; Iatrou, H.; Hadjichristidis, N. Radius of gyration of polystyrene combs and centipedes in solution. *Macromolecules* **2000**, *33* (22), 8323−8328.

(4) (a) Flat, J. J. New Comb-Like Nanostructured Copolymers: A Promising Route Towards New Industrial Applications. *Polym. Degrad.*

Stab. **2007**, *92* (12), 2278−2286. (b) Feng, C.; Li, Y.; Yang, D.; Hu, J.; Zhang, X.; Huang, X. Well-Defined Graft Copolymers: From Controlled Synthesis to Multipurpose Applications. *Chem. Soc. Rev.* **2011**, *40* (3), 1282−1295. (c) Xie, G.; Martinez, M. R.; Olszewski, M.; Sheiko, S. S.; Matyjaszewski, K. Molecular bottlebrushes as novel materials. *Biomacromolecules* **2019**, *20* (1), 27−54.

(5) Feng, C.; Huang, X. Polymer brushes: efficient synthesis and applications. *Acc. Chem. Res.* **2018**, *51* (9), 2314−2323.

(6) Giacomelli, C.; Schmidt, V.; Aissou, K.; Borsali, R. Block Copolymer Systems: From Single Chain to Self-Assembled Nanostructures. *Langmuir* **2010**, *26* (20), 15734−15744.

(7) (a) Tritschler, U.; Pearce, S.; Gwyther, J.; Whittell, G. R.; Manners, I. 50th anniversary perspective: Functional nanoparticles from the solution self-assembly of block copolymers. *Macromolecules* **2017**, *50* (9), 3439−3463. (b) Karayianni, M.; Pispas, S. Block copolymer solution self-assembly: Recent advances, emerging trends, and applications. *J. Polym. Sci.* **2021**, *59* (17), 1874−1898. (c) Deng, Z.; Liu, S. Emerging trends in solution self-assembly of block copolymers. *Polymer* **2020**, *207*, 122914.

(8) Theato, P.; Sumerlin, B. S.; O'Reilly, R. K.; Epps III, T. H., III Stimuli responsive materials. *Chem. Soc. Rev.* **2013**, *42* (17), 7055−7056.

(9) (a) Roy, D.; Brooks, W. L.; Sumerlin, B. S. New directions in thermoresponsive polymers. *Chem. Soc. Rev.* **2013**, *42* (17), 7214−7243. (b) Qiao, S.; Wang, H. Temperature-responsive polymers: Synthesis, properties, and biomedical applications. *Nano Res.* **2018**, *11* (10), 5400−5423. (c) Ward, M. A.; Georgiou, T. K. Thermoresponsive polymers for biomedical applications. *Polymers* **2011**, *3* (3), 1215−1242. (d) Sponchioni, M.; Capasso Palmiero, U.; Moscatelli, D. Thermo-responsive polymers: Applications of smart materials in drug delivery and tissue engineering. *Mater. Sci. Eng., C* **2019**, *102*, 589−605.

(10) Hoogenboom, R. Poly(2-oxazoline)s: a polymer class with numerous potential applications. *Angew. Chem., Int. Ed.* **2009**, *48* (43), 7978−7994.

(11) (a) Weber, C.; Krieg, A.; Paulus, R. M.; Lambermont-Thijs, H. M. L.; Becer, C. R.; Hoogenboom, R.; Schubert, U. S. Thermal Properties of Oligo(2-ethyl-2-oxazoline) Containing Comb and Graft Copolymers and their Aqueous Solutions. *Macromol. Symp.* **2011**, *308* (1), 17−24. (b) Bloksma, M. M.; Weber, C.; Perevyazko, I. Y.; Kuse, A.; Baumgartel, A.; Vollrath, A.; Hoogenboom, R.; Schubert, U. S. Poly(2-cyclopropyl-2-oxazoline): from rate acceleration by cyclopropyl to thermoresponsive properties. *Macromolecules* **2011**, *44* (11), 4057−4064. (c) Floyd, T. G.; Hakkinen, S.; Hall, S. C. L.; Dalgliesh, R. M.; Lehnen, A. C.; Hartlieb, M.; Perrier, S. Cationic Bottlebrush Copolymers from Partially Hydrolyzed Poly(oxazoline) s. *Macromolecules* **2021**, *54* (20), 9461−9473. (d) Yildirim, I.; Bus, T.; Sahn, M.; Yildirim, T.; Kalden, D.; Hoeppener, S.; Traeger, A.; Westerhausen, M.; Weber, C.; Schubert, U. S. Fluorescent amphiphilic heterografted comb polymers comprising biocompatible PLA and PEtOx side chains. *Polym. Chem.* **2016**, *7* (39), 6064−6074. (e) Weber, C.; Remzi Becer, C.; Guenther, W.; Hoogenboom, R.; Schubert, U. S. Dual responsive methacrylic acid and oligo(2-ethyl-2-oxazoline) containing graft copolymers. *Macromolecules* **2010**, *43* (1), 160−167. (f) Weber, C.; Becer, C. R.; Hoogenboom, R.; Schubert, U. S. Lower critical solution temperature behavior of comb and graft shaped poly [oligo(2-ethyl-2-oxazoline)methacrylate] s. *Macromolecules* **2009**, *42* (8), 2965−2971.

(12) (a) Zhang, N.; Huber, S.; Schulz, A.; Luxenhofer, R.; Jordan, R. Cylindrical molecular brushes of poly (2-oxazoline) s from 2-isopropenyl-2-oxazoline. *Macromolecules* **2009**, *42* (6), 2215−2221. (b) Weber, C.; Neuwirth, T.; Kempe, K.; Ozkahraman, B.; Tamahkar, E.; Mert, H.; Becer, C. R.; Schubert, U. S. 2-Isopropenyl-2-oxazoline: A versatile monomer for functionalization of polymers obtained via RAFT. *Macromolecules* **2012**, *45* (1), 20−27. (c) Zhang, N.; Salzinger, S.; Soller, B. S.; Rieger, B. Rare earth metal-mediated group-transfer polymerization: from defined polymer microstructures to high-precision nano-scaled objects. *J. Am. Chem. Soc.* **2013**, *135* (24), 8810−8813. (d) Beyer, V. P.; Cattoz, B.; Strong, A.; Schwarz, A.; Becer, C. R. Brush copolymers from 2-oxazoline and acrylic monomers via an inimer approach. *Macromolecules* **2020**, *53* (8), 2950−2958. (e) Kim, J.; Waldron, C.; Cattoz, B.; Becer, C. R. An ϵ-caprolactone-derived 2-oxazoline inimer for the synthesis of graft copolymers. *Polym. Chem.* **2020**, *11* (42), 6847−6852. (f) Kim, J.; Cattoz, B.; Leung, A. H. M.; Parish, J. D.; Becer, C. R. Enabling Reversible Addition-Fragmentation Chain-Transfer Polymerization for Brush Copolymers with a Poly(2-oxazoline) Backbone. *Macromolecules* **2022**, *55*, 4411−4419.

(13) Concilio, M.; Nguyen, N.; Becer, C. R. Oxazoline-Methacrylate Graft-Copolymers with Upper Critical Solution Temperature Behaviour in Yubase Oil. *Polym. Chem.* **2021**, *12* (30), 4359−4371.

(14) (a) Rayeroux, D.; Travelet, C.; Lapinte, V.; Borsali, R.; Robin, J. J.; Bouilhac, C. Tunable amphiphilic graft copolymers bearing fatty chains and polyoxazoline: synthesis and self-assembly behavior in solution. *Polym. Chem.* **2017**, *8* (29), 4246−4263. (b) Morgese, G.; Cavalli, E.; Rosenboom, J. G.; Zenobi-Wong, M.; Benetti, E. M. Cyclic polymer grafts that lubricate and protect damaged cartilage. *Angew. Chem.* **2018**, *130* (6), 1637−1642. (c) Le Fer, G.; Le Cœur, C.; Guigner, J. M.; Amiel, C.; Volet, G. Self-assembly of poly(2-alkyl-2-oxazoline-)-g-poly(D,L-lactide) copolymers. *Eur. Polym. J.* **2017**, *88*, 656−665.

(15) Halacheva, S.; Price, G. J.; Garamus, V. M. Effects of temperature and polymer composition upon the aqueous solution properties of comblike linear poly(ethylene imine)/poly(2-ethyl-2-oxazoline)-based polymers. *Macromolecules* **2011**, *44* (18), 7394−7404.

(16) (a) Kaberov, L. I.; Verbraeken, B.; Hruby, M.; Riabtseva, A.; Kovacik, L.; Kereiche, S.; Brus, J.; Stepanek, P.; Hoogenboom, R.; Filippov, S. K. Novel triphilic block copolymers based on poly(2-methyl-2-oxazoline)−block−poly(2-octyl-2-oxazoline) with different terminal perfluoroalkyl fragments: Synthesis and self-assembly behaviour. *Eur. Polym. J.* **2017**, *88*, 645−655. (b) Wang, Y.; Zhang, B.; Shen, X.; Li, Q.; Su, F.; Li, S. Biocompatibility, drug release, and anti-tumor effect of pH-sensitive micelles prepared from poly(2-ethyl-2-oxazoline)-poly(DL-lactide) block copolymers. *Polym. Adv. Technol.* **2021**, *32* (10), 4142−4152.

(17) Milonaki, Y.; Kaditi, E.; Pispas, S.; Demetzos, C. Amphiphilic gradient copolymers of 2-methyl-and 2-phenyl-2-oxazoline: self-organization in aqueous media and drug encapsulation. *J. Polym. Sci. A Polym. Chem.* **2012**, *50* (6), 1226−1237.

(18) (a) Daubian, D.; Gaitzsch, J.; Meier, W. Synthesis and complex self-assembly of amphiphilic block copolymers with a branched hydrophobic poly(2-oxazoline) into multicompartment micelles, pseudo-vesicles and yolk/shell nanoparticles. *Polym. Chem.* **2020**, *11* (6), 1237−1248. (b) Daubian, D.; Fillion, A.; Gaitzsch, J.; Meier, W. One-pot synthesis of an amphiphilic ABC triblock copolymer PEO-b-PEHOx-b-PEtOz and its self-assembly into nanoscopic asymmetric polymersomes. *Macromolecules* **2020**, *53* (24), 11040−11050.

(19) Hoogenboom, R.; Schlaad, H. Thermoresponsive poly(2-oxazoline) s, polypeptoids, and polypeptides. *Polym. Chem.* **2017**, *8* (1), 24−40.

(20) Anas, M.; Jana, S.; Mandal, T. K. Vesicular assemblies of thermoresponsive amphiphilic polypeptide copolymers for guest encapsulation and release. *Polym. Chem.* **2020**, *11* (16), 2889−2903.

(21) Bose, A.; Jana, S.; Saha, A.; Mandal, T. K. Amphiphilic polypeptide-polyoxazoline graft copolymer conjugate with tunable thermoresponsiveness: Synthesis and self-assembly into various micellar structures in aqueous and nonaqueous media. *Polymer* **2017**, *110*, 12−24.

(22) Wu, X.; Qiao, Y.; Yang, H.; Wang, J. Self-assembly of a series of random copolymers bearing amphiphilic side chains. *J. Colloid Interface Sci.* **2010**, *349* (2), 560−564.

(23) Zhu, X.; Liu, M. Self-assembly and morphology control of new l-glutamic acid-based amphiphilic random copolymers: Giant vesicles, vesicles, spheres, and honeycomb Film. *Langmuir* **2011**, *27* (21), 12844−12850.

(24) (a) Stephan, T.; Muth, S.; Schmidt, M. Shape changes of statistical copolymacromonomers: From wormlike cylinders to horse-shoe-and meanderlike structures. *Macromolecules* **2002**, *35* (27), 9857−9860. (b) Sun, G.; Zhang, M.; He, J.; Ni, P. Synthesis of amphiphilic cationic copolymers poly[2-(methacryloyloxy) ethyl trimethylammonium chloride-co-stearyl methacrylate] and their self-assembly

https://doi.org/10.1021/acs.macromol.3c01308
Macromolecules 2023, 56, 7961−7972

behavior in water and water-ethanol mixtures. *J. Polym. Sci. A Polym. Chem.* **2009**, *47* (18), 4670−4684.
(25) Ilhan, F.; Galow, T. H.; Gray, M.; Clavier, G.; Rotello, V. M. Giant vesicle formation through self-assembly of complementary random copolymers. *J. Am. Chem. Soc.* **2000**, *122* (24), 5895−5896.
(26) Liu, X.; Kim, J. S.; Wu, J.; Eisenberg, A. Bowl-shaped aggregates from the self-assembly of an amphiphilic random copolymer of poly (styrene-co-methacrylic acid). *Macromolecules* **2005**, *38* (16), 6749−6751.
(27) Pitsikalis, M. Ionic Polymerization. *Reference Module in Chemistry, Molecular Sciences and Chemical Engineering*, 2013. (b) Uchida, S. Graft Copolymer Synthesis. In *Encyclopedia of Polymeric Nanomaterials*; Kobayashi, S., Müllen, K., Eds.; Springer, 2015; pp 867−870.
(28) Lin, P.; Clash, C.; Pearce, E. M.; Kwei, T. K.; Aponte, M. A. Solubility and miscibility of poly(ethyl oxazoline). *J. Polym. Sci. B Polym. Phys.* **1988**, *26* (3), 603−619.
(29) (a) Seno, K. I.; Date, A.; Kanaoka, S.; Aoshima, S. Synthesis and solution properties of poly (vinyl ether) s with long alkyl chain, biphenyl, and cholesteryl pendants. *J. Polym. Sci. A Polym. Chem.* **2008**, *46* (13), 4392−4406. (b) Yoshida, T.; Seno, K. I.; Kanaoka, S.; Aoshima, S. Stimuli-Responsive Reversible Physical Networks. I. Synthesis and Physical Network Properties of Amphiphilic Block and Random Copolymers with Long Alkyl Chains by Living Cationic Polymerization. *J. Polym. Sci. Part A Polym. Chem.* **2005**, *43* (6), 1155−1165.
(30) Derry, M. J.; Fielding, L. A.; Armes, S. P. Polymerization-induced self-assembly of block copolymer nanoparticles via RAFT non-aqueous dispersion polymerization. *Prog. Polym. Sci.* **2016**, *52*, 1−18.
(31) Fielding, L. A.; Lane, J. A.; Derry, M. J.; Mykhaylyk, O. O.; Armes, S. P. Thermo-Responsive Diblock Copolymer Worm Gels in Non-Polar Solvents. *J. Am. Chem. Soc.* **2014**, *136* (15), 5790−5798.

https://doi.org/10.1021/acs.macromol.3c01308
Macromolecules 2023, 56, 7961−7972